BENCHMARKING CLIMATE MODEL TOP-OF-ATMOSPHERE RADIANCE IN THE 9.6μm OZONE BAND COMPARED TO TES AND IASI OBSERVATIONS

Helen Worden, Andrew Conley, Jean-François Lamarque, Steve Massie (NCAR), Kevin Bowman, Le Kuai (JPL), Drew Shindell, Greg Falvegi (Duke Univ.), Cathy Clerbaux, (LATMOS), Pierre-François Coheur, Stamatia Doniki (ULB), William Collins (UCB), Andrew Lacis (GISS)

The Problem

This work addresses two primary questions:

1) What is the bias in IPCC climate model predictions of present day top-of-atmosphere (TOA) flux in the 9.6μm ozone band?

2) What is the impact of an ozone band TOA flux bias on present day tropospheric ozone flux sensitivity and pre-industrial to present day ozone radiative forcing estimates?

Large range in model estimates for:

Direct Ozone RF

- Preindustrial-to-present day: 0.35 W/m² [0.25 to 0.65 W/m²]
- through 21st century: 0.89 W/m²

Biases in the IR ozone band TOA flux and flux sensitivity will be tested with CAM-chem, RRTMG and GISS radiative transfer (RT) models using TES and IASI TOA flux and IRKs.

Climate RT Model	Institution	Ozone bands (cm^{-1})	References
CAM-RT (band)	NCAR	1000-1120	Lamarque et al., JGR, 2008 Conley et al., GMD, 2013
CAM-RRTMG (correlated-k)	NCAR/AER	980-1080	Iacono et al., JGR, 2008
GISS-RT (band)	GISS/Duke Univ.	970-1010, 1010-1070, 1070-1210*	Schmidt et al., J. Clim. 2006 Shindell et al., ACP, 2013

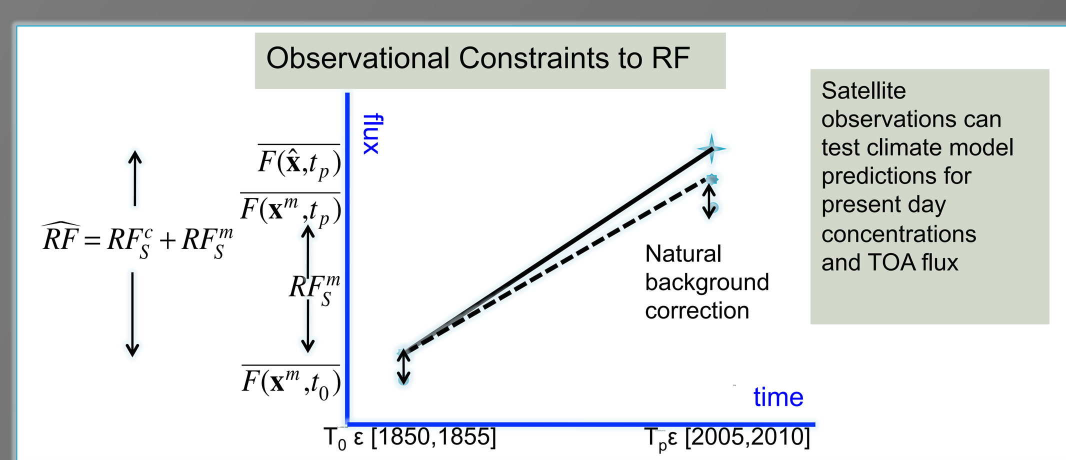

TOA long-wave ozone band flux

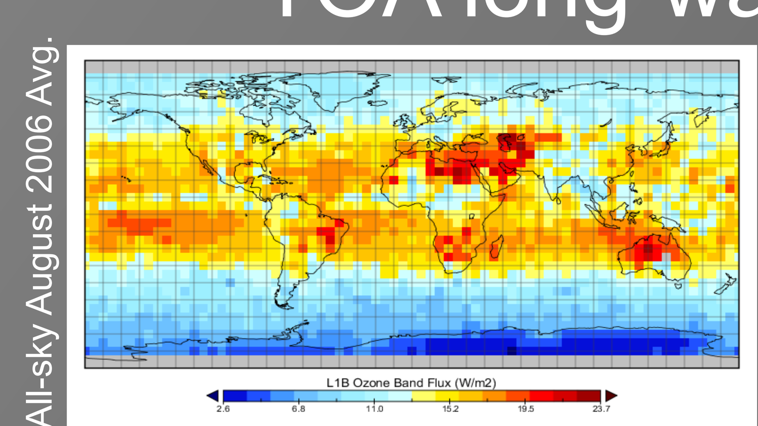

TES TOA flux (F_{TOA}) for August 2006

- Similar to OLR but only for the IR ozone band
- This is a fundamental quantity, predicted by climate models, but never tested against observations.

Known issues:

- RRTMG band is 980-1080; TES band is 985-1080 (~1.1 to 1.7 W/m² difference)
- RRTMG-corrected adjusts for this difference in frequency range.
- Different estimate of anisotropy
- Assumptions for water vapor in RRTMG
- scatter not due to TES noise (0.1% for flux)

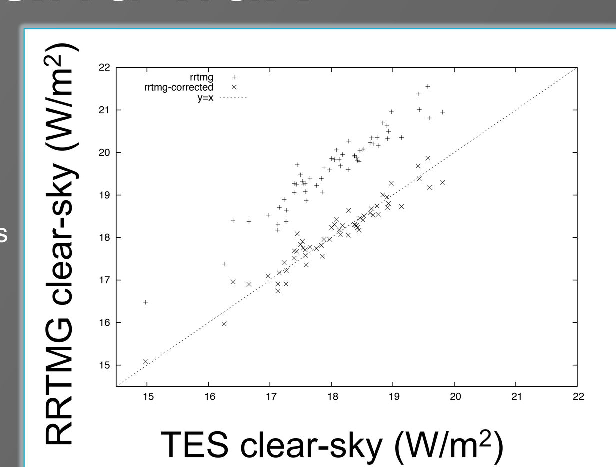

O_3 band flux comparison with RRTMG for atmospheres specified from TES

What TES and IASI measure

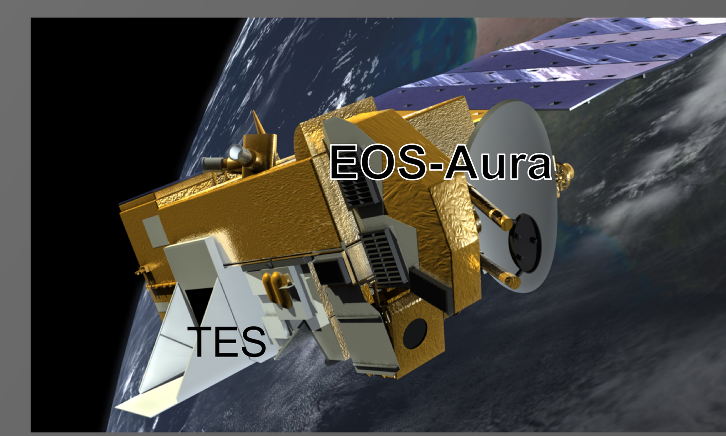

	TES	IASI
Instrument	FTS	FTS
Spectral resolution	0.1 cm^{-1}	0.5 cm^{-1}
Spectral coverage	652 to 2251 cm^{-1}	645 to 2760 cm^{-1}
NeΔT	0.30K @ 300 K	0.15K @ 280K
Footprint size	8.5 x 5.3 km²	12km diameter
Sampling coverage	Sparse global coverage (16 days)	global coverage twice per day
Orbit alt.	705 km	817 km
Eq. x-ing	13:30 LST	9:30 LST

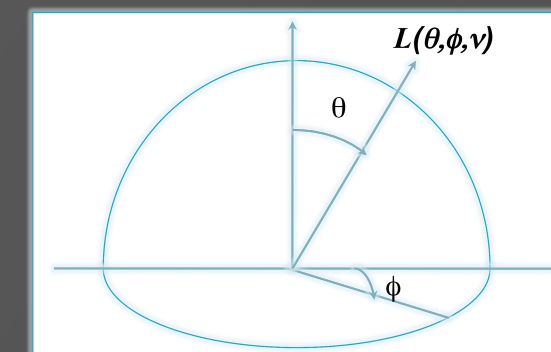

$$F_{TOA} = \int d\nu \int_0^{2\pi}\int_0^{\frac{\pi}{2}} L_\nu(\theta)\cos\theta\sin\theta\, d\theta\, d\phi$$

$$IRK = \frac{\partial F_{TOA}}{\partial q_l} \qquad LIRK = \frac{\partial F_{TOA}}{\partial \ln q_l}$$

$$LWRE = \Delta F_{TOA} = \sum_{l=surface}^{tropopause} \left(\frac{\partial F_{TOA}}{\partial q_l}\right) q_l$$

$L(\theta,\phi,\nu)$ = TOA Radiance (W/cm²/sr/cm⁻¹)

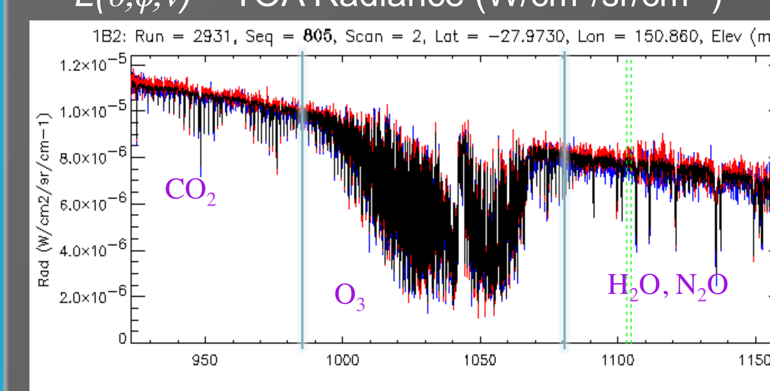

Example of TES spectral radiance used to retrieve O_3 vertical profiles.

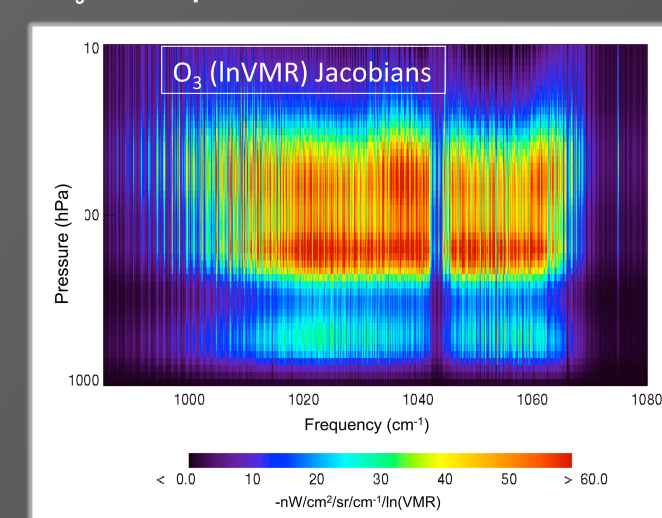

Example of TES Jacobian matrix used in O_3 retrieval and for O_3 IRKs.

$$\frac{\partial L_{TOA}(\nu)}{\partial q_l} = \frac{1}{q_l}\frac{\partial L_{TOA}(\nu)}{\partial \ln q_l}$$

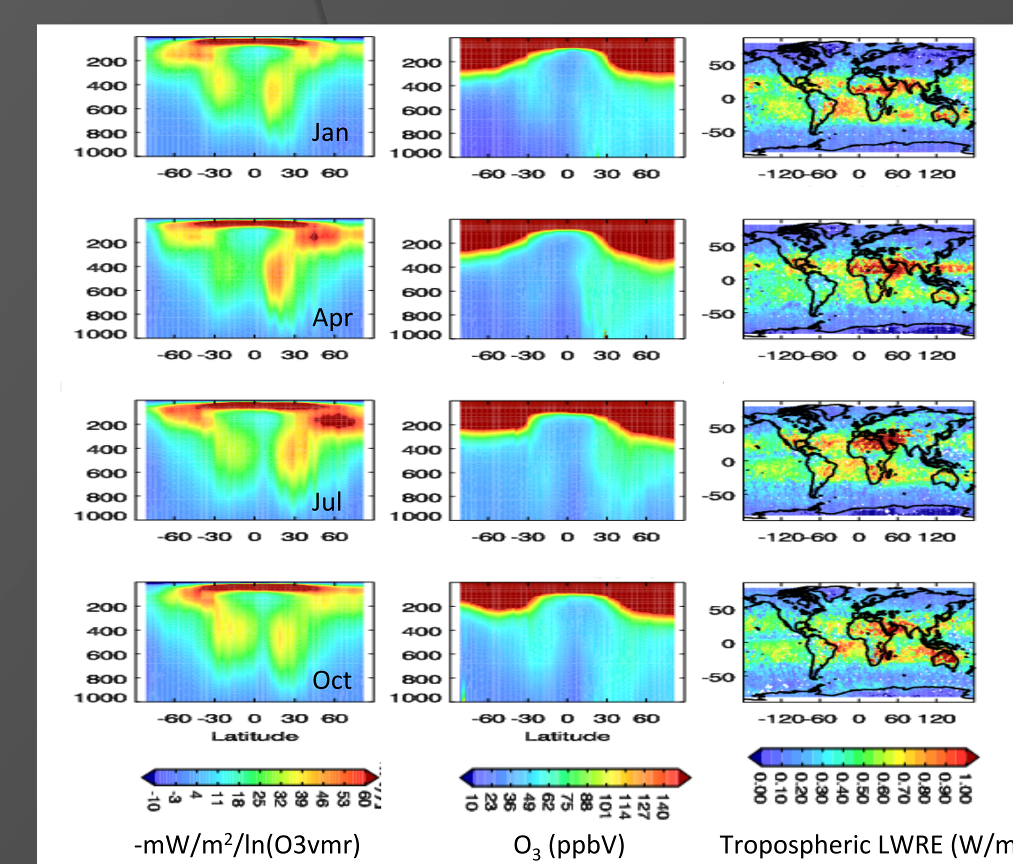

TES monthly averages for LIRK, O3 and LWRE

IRK: Instantaneous Radiative Kernel

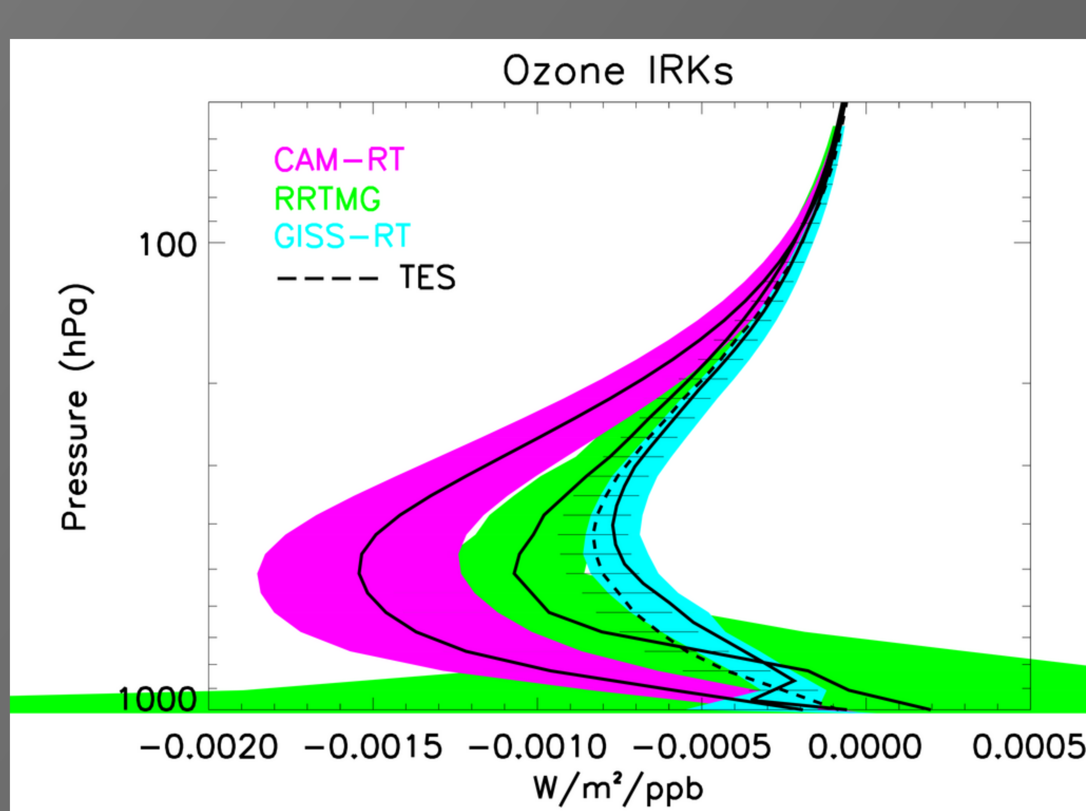

Model and TES average IRKs with standard deviations indicated by color spread (models) and bars (TES). Models calculations used atmospheric state corresponding to TES data, 2011.07.15 from 81 cloud-free ocean observations, 29°S – 48°N

LWRE: Long-Wave Radiative Effect

Comparisons of model LWRE to TES for same atmospheric states

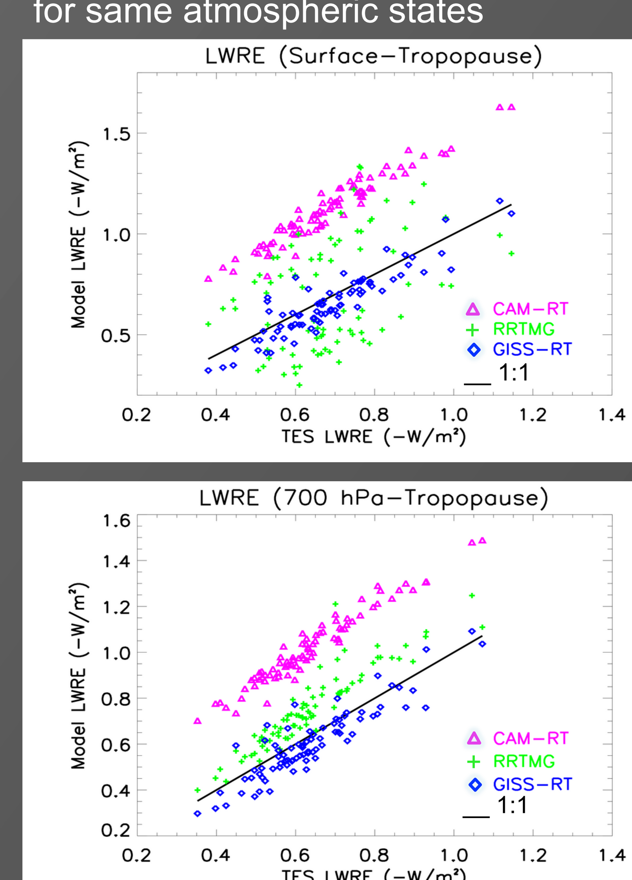

Model	Correlation R^2	Slope	Offset
CAM-RT	0.97	1.13	-0.30
RRTMG	0.92	1.17	-0.01
GISS-RT	0.91	1.00	0.04

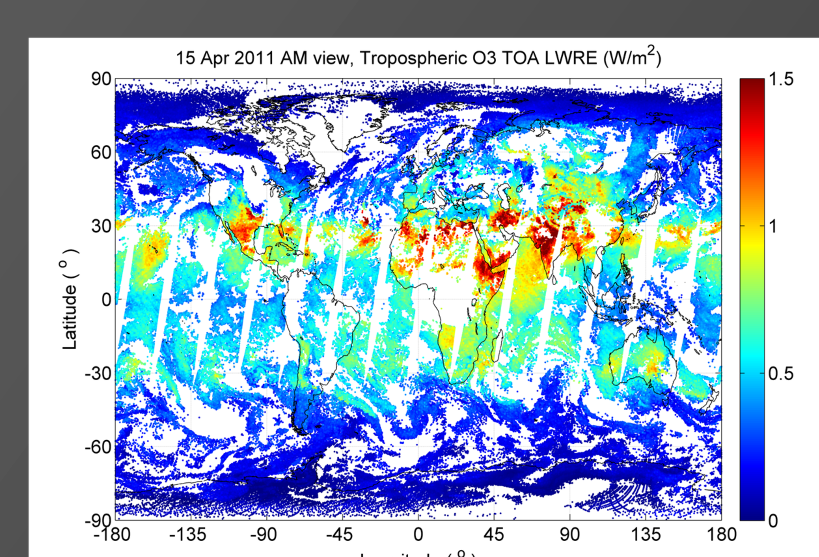

Tropospheric O3 LWRE from IASI on MetOp-A for a single day of observations (day only). White areas indicate clouds and measurement gaps.

IASI and TES now apply same methods for calculating IRKs:

- Direct integration of Jacobians with 5-angle Gaussian integration described in Doniki et al., ACPD, 2015. (Used in all results shown here)
- Older TES IRK computation applied less accurate single–angle anisotropy estimate and neglected partial derivative of anisotropy to ozone.

IASI-TES LWRE comparisons

- IASI=TES±0.5° lat/lon
- 6 hour time diference

Tropospheric O_3 LWRE

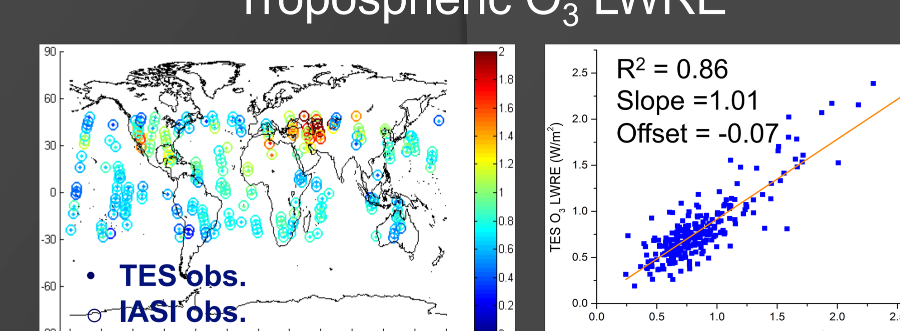

TOA total column O_3 LWRE

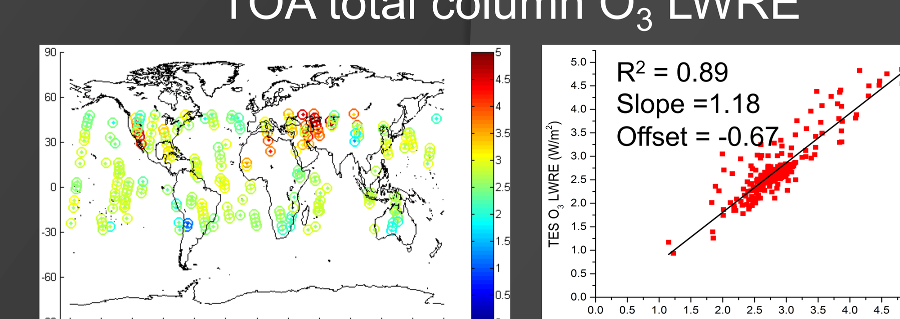

Ozone and Water Vapor radiative coupling

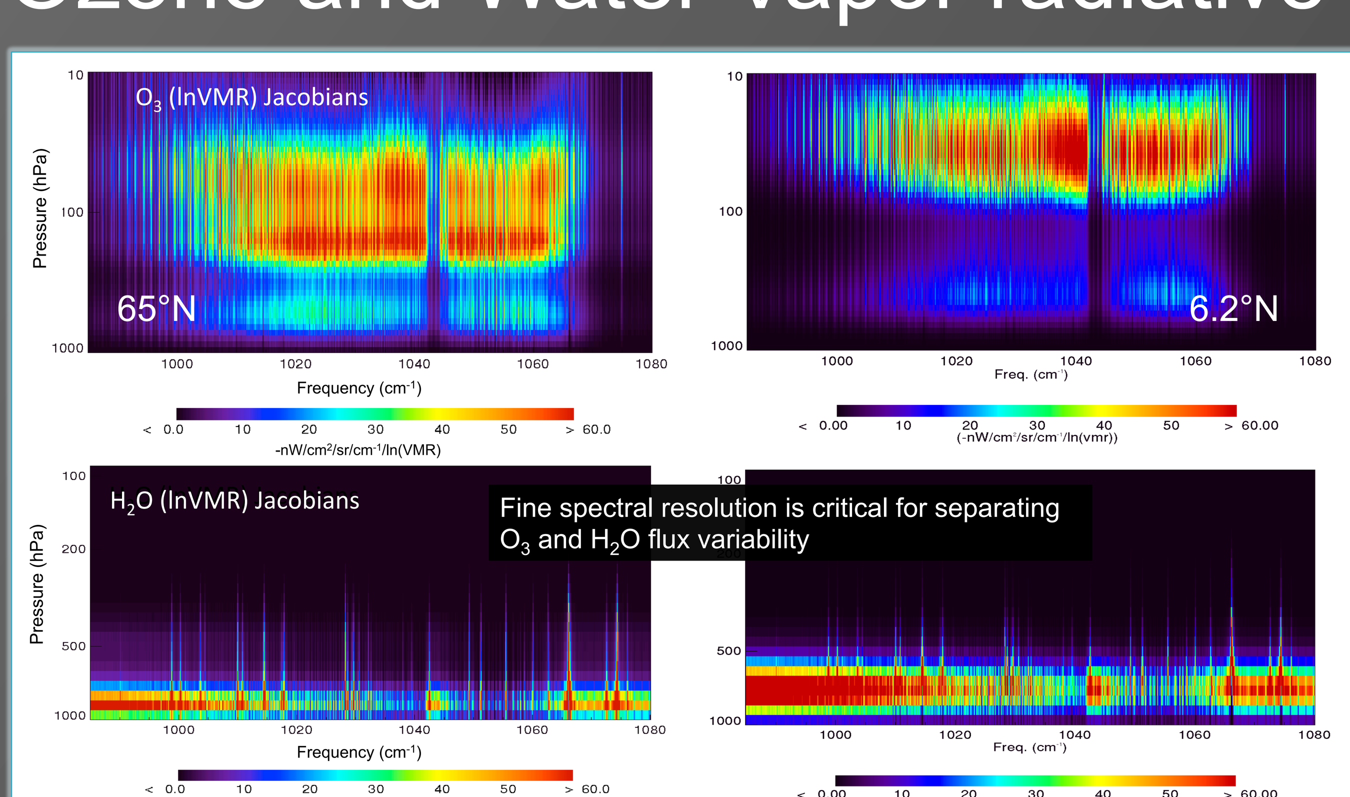

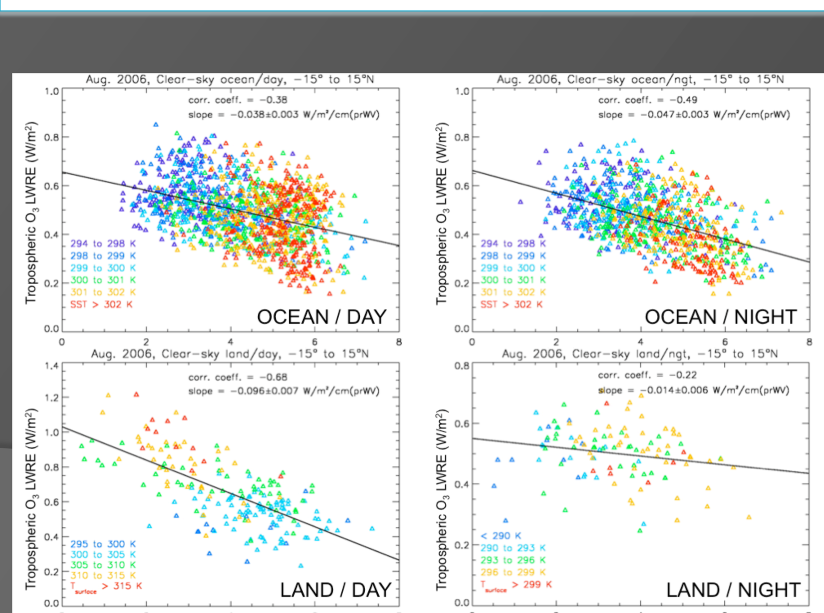

Worden et al., JGR, 2011

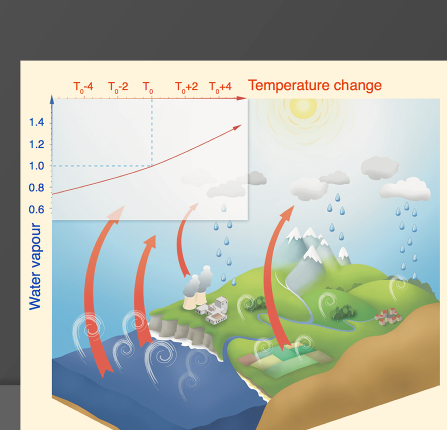

IPCC AR5 FAQ 8.1 Fig. 1: Water cycle with water vapour feedback ~7%/°C

Water vapor LWRE in the IR ozone band

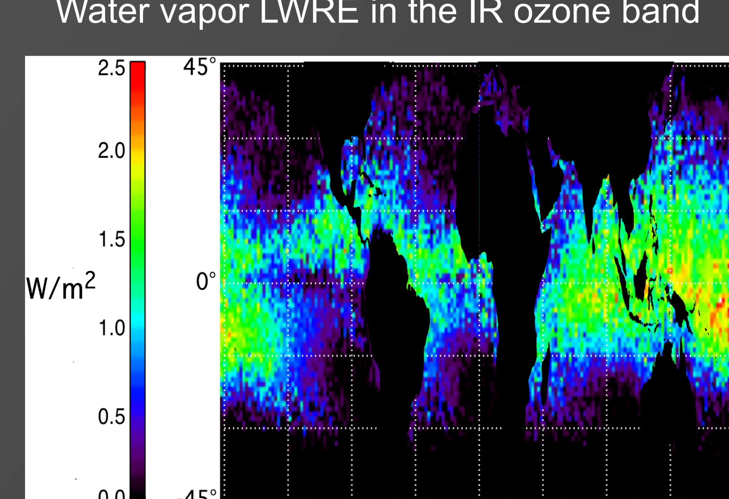

Worden et al., Nature GEO, 2008

Attribution of bias in O_3 LWRE due to model/data differences in atmospheric state:

Fasullo and Trenberth [2012] showed that IPCC models overestimated relative humidity in the tropical subsidence regions, which was directly related to how the models predicted global mean surface temperature change from a doubling of CO2 (i.e., climate sensitivity). Therefore, we could expect that IPCC chemistry-climate models will have a biased atmospheric state in the tropical subsidence region, which will then lead to biases in the model LWRE due to atmospheric opacity and consequently ozone radiative forcing.

New TES research products to examine O_3 RF feedbacks and bias:

$$\frac{\partial F_{OzoneBand}}{\partial H_2O}, \frac{\partial F_{OzoneBand}}{\partial T_{atmos.}}, \frac{\partial F_{OzoneBand}}{\partial T_{surface}}, \frac{\partial F_{OzoneBand}}{\partial OD_{cloud}}, \frac{\partial F_{OzoneBand}}{\partial P_{cloudTop}}$$

Conclusions

- TOA flux from the IR Ozone band is a fundamental quantity in climate models that has not been compared to measurements.
- Continuing the TES record with IASI data is critical for understanding present day to future changes in O_3 radiative forcing, such as cloud coverage and water vapor feedback.
- Initial results show differences for both flux (~2% RRTMG-TES) and flux sensitivity (CAM-RT ~2 x TES, large spread near surface in RRTMG) between models and data that need to be reconciled.

IRK References

Doniki, S., et al.: Instantaneous longwave radiative impact of ozone: an application on IASI/MetOp observations, Atmos. Chem. Phys. Discuss., 15, 21177-21218, doi:10.5194/acpd-15-21177-2015, 2015.

Bowman, K. W., et al.: Evaluation of ACCMIP outgoing longwave radiation from tropospheric ozone using TES satellite observations, ***Atmospheric Chemistry and Physics****, 13, 4057–4072, 2013*, doi:10.5194/acp-13-4057-2013. (2013)

Bowman, K. W. and D. K. Henze: Attribution of direct ozone radiative forcing to spatially resolved emissions, ***Geophysical Research Letters****, VOL. 39, L22704*, doi:10.1029/2012GL053274, (2012)

Aghedo, A.M., et al.:The vertical distribution of ozone instantaneous radiative forcing from satellite and chemistry climate models, ***Journal of Geophysical Research****, Vol. 116, No. D1, D01305*, doi:10.1029/2010JD014243 (2011)

Worden, H.M., et al.: Sensitivity of outgoing longwave radiative flux to the global vertical distribution of ozone characterized by instantaneous radiative kernels from Aura-TES, ***Journal of Geophysical Research****, 116, D14115*, doi: 10.1029/2010JD015101 (2011)

Worden, H. M., K. W. Bowman, J. R. Worden, A. Eldering and R. Beer, Satellite measurements of the clear-sky greenhouse effect from tropospheric ozone, ***Nature Geoscience***, doi:10.1038/ngeo182, (2008)

http://tes.jpl.nasa.gov/

http://smsc.cnes.fr/IASI/